DISSEMINATION OF KNOWLEDGE

International Journal of Artificial Intelligence and Machine Learning

Publisher's Home Page: https://www.svedbergopen.com/

Research Paper Open Access

# A Novel Medical Image Fusion Approach Using Local Features And Deep Learning In Wavelet Domain

Sreelakshmi A N[1], N. Sujatha[2]

[1]Research Scholar, P.G & Research Department of Computer Science, Sri Meenakshi Govt. Arts College for Women (Autonomous), Madurai Kamaraj University, Madurai, Tamilnadu, India.

[2]Associate Professor, P.G & Research Department of Computer Science, Sri Meenakshi Govt. Arts College for Women (Autonomous), Madurai Kamaraj University, Madurai, Tamilnadu, India. Email: sree.an1989@gmail.com

**Abstract**

In clinical evaluation, medical image analysis is essential. Computed Tomography (CT) and Magnetic Resonance Imaging (MRI) are widely utilized in the medical sector for disease diagnosis. However, extracting the necessary information to detect suspicious tissue features from a single image is quite challenging. Multimodal image fusion has garnered increased interest because it allows physicians to view multiple modalities in one image. Physicians can accurately diagnose diseases and effectively plan treatment by analyzing the fused image. Numerous techniques have been devoted to image fusion. However, the fused images have issues with brightness, contrast, and noise, making it difficult to precisely analyze the images. To tackle these issues, this paper introduces a new Medical Image Fusion (MIF) method based on Wavelet Transform (WT) and Deep Convolutional Neural Network (DCNN). The key objective of the proposed method is to maintain diagnostic data in the fused image. The introduced method applies WT on source images to divide approximate and detail subbands. Approximation subbands are fused using local features. Detail subbands are denoised using an improved thresholding method and then fused utilizing DCNN. After fusion, inverse WT is employed to obtain the final fused image. MRI and CT scans from the The effectiveness of the suggested approach is verified using Brain Atlas. Experimental outcomes highlight the superior performance of the proposed model when compared to recent medical image fusion approaches.

**Keyword:** Medical image fusion, Deep convolutional neural network, Wavelet transform, Local features, Diagnosis.

## INTRODUCTION

With the rapid developments in sensor and computer technology, medical image analysis is essential for many areas of disease diagnosis, such as treatment planning, surgery, and monitoring of serious diseases [1]. However, diagnosis accuracy heavily dependent on visual quality and are relevant features. Nowadays, several imaging techniques such as Computed Tomography (CT), Magnetic Resonance Imaging (MRI), and Position Emission Tomography (PET) are used to visualize and capture a specific organ for diagnostic purposes. Each type of medical image provides different information [2]. It dissipates the information and makes the physician's decision-making more difficult. This challenge has drawn significant attention from researchers in medical image diagnosis [3]. To solve such an issue, the concept of image fusion has emerged as an effective solution.

Image fusion is the process of combining two or more images to create a new one that is understandable and instructive in every area (IF) [4],[5]. The process of multimodal image fusion enhances the quality and clinical value of medical images by merging key elements from several images obtained using distinct imaging modalities [6]. Over the years, Various techniques for combining medical images have been created. These techniques may be divided into four categories: machine learning (ML) techniques [9], hybrid techniques [10], frequency domain techniques [7], and spatial domain techniques [8]. Spatial domain techniques directly modify the pixels of the source images to produce a fused image. Transform domain-based approaches use different transforms like wavelet transform (WT), and curvelet transform to merge two images. Although transform-based methods often provide better visual quality and preserve diagnostic details, they may experience fused image artifacts around the edges.

ML-based approaches have the power to alleviate these problems more effectively [11]. Deep Learning (DL) [13] based techniques have drawn a lot of interest lately, yet using DL directly in the spatial domain causes prominent characteristics to be lost. To overcome this problem, scientists have created hybrid approaches that combine the best features of many areas. However, the low contrast, illumination, and edge loss in the merged image detract from it.

In this context, this paper aims to address these gaps by introducing a new IF framework that solves the mentioned shortcomings. This research presents a Deep Convolutional Neural Network (DCNN) and WT-based Medical Image Fusion (MIF) technique. This is the first time, as far as the author is aware, that the proposed approach makes use of WT and DCNN. In this approach, approximation subbands are merged using local features, and detail subbands are fused with DCNN. The suggested technique successfully combines medical images. Clear and accurate diagnostic information from the source images is included in the fused image. The following are the paper's main contributions:

- A novel MIF method is proposed by integrating WT and DL for efficient image fusion.
- WT is used for separating source images into subbands that are approximate and detailed.
- Improved wavelet thresholding is used to remove redundant data from the subbands.
- Approximation subbands are fused based on local features and detail subbands are merged using the DCNN.
- To get the ultimate fused image, inverse WT is applied to the fused subbands.
- The suggested fusion technique uses WT and DL to maintain the diagnostic data from the combined CT and MRI images in the fused image.
- The scalability of the method is verified using data from Brain Atlas data.
- The suggested strategy outperforms earlier techniques, as shown by both objective evaluation and visual perception.

The following summarizes the remainder of the article. The second section talks about modern IF methods. The suggested MIF approach is explained in Section 3. A discussion and numerical findings are presented in Section 4. The conclusion and future scopes are included in Section 5.

## Related works

The IF has played a pivotal role in the medical field due to its applications such as automated diagnosis, and analysis of serious disease and trauma. Utilizing a variety of techniques, several researchers have attempted to increase the combined image quality. However, there is still room for improvement.

Sandhya et al. [3] designed a hybrid model to fuse CT and MRI images. The proposed method used Shearlet Transform (ST) and Principal Component Analysis (PCA). The process involved transforming medical images using ST and then applying PCA to these images. Inverse ST was used to generate the fused image. However, this method suffers from spectral distortion. The decomposition-based IF method was utilized in [4], which effectively restores edge details. In this approach, Variational Mode Decomposition (VMD) was applied to the source images to divide into multiple intrinsic mode functions. These functions were combined with local energy maxima.

Dogra and Kumar proposed a hybrid fusion approach based on statistics and ST [5]. ST divided source images into basic and detail layers. A guided image filter and image statistics fusion rule fused base layers, whereas the max fusion rule fused dense layers. The final fused image was obtained using inverse ST. This approach preserves texture features. Tawfik et al. [6] developed a hybrid pixel-feature-based approach to merge medical image combinations. To get Low-frequency (LF) and High-frequency (HF) coefficients for pixel fusion, WT was applied to the source images. LF coefficients were merged using the max fusion rule, while HF coefficients were merged using PCA. For feature-level fusion, various features were computed from LF and HF and then fused. The final image was reconstructed using inverse DWT. However, this approach requires more time for fusion.

An interesting approach using DL for IF was introduced by Bhutto et al. [9]. The authors used the bottom-hat-top-hat technique to suppress noise. They divided images into LF and HF with ST. LF bands were fused using local energy and HF bands were merged using Siamese CNN (SCNN). Singh et al. [10] presented a comprehensive survey of IF methods along with their strength and weaknesses. Kaur and Singh [11] implemented a deep neural network for medical image fusion. Source images were divided into subbands via Non-subsampled Contourlet Transform (NSCT). Following this, Xception was employed to compute features from source images. Optimal features were chosen using a differential evolution algorithm.

He et al. [12] attempted to improve the quality of fused images with Pulse Coupled Neural Network (PCNN). The authors combined region-based level partition with PCNN to combine two images. Nevertheless, this approach requires fine-tuning of parameters to achieve satisfactory results. Odusami et al. [13] used Resnet to integrate MRI and PET for precise diagnosis. The network was designed and trained using images to get the desired results. Rallabandi et al. [14] developed a fusion model combining MRI and PET images. The process involved decomposing source images into LF and HF coefficients using DWT. While the minimum rule was employed to fuse the HF components, the average rule was utilized to fuse the LF components. Inverse DWT was employed to reconstruct the fused image.

Qiu et al. [15] introduced a model named hierarchical Attention Mechanism (AM) to fuse medical images for disease diagnosis. This approach used a supervised model and AM for extracting features from the source image and fusion, respectively. This approach provided better results with high computational overhead. A multimodal image fusion based on Hybrid Attention Mechanism (HAM) was presented by Wei and Ji [16]. The HAM approaches fused source images by exploring shared information between two images. Although this approach provided better results, the quality of the image was very poor. Shilpa et al. [17] used an enhanced JAYA optimization algorithm to fuse medical images. The authors adopted Non-subsampled ST (NSST) to decompose images into LF and HF bands. EJAYA algorithm was used to obtain weights for merging HF bands. LF bands were combined using the max fusion rule.

Sale [19] presented a spatial domain approach for image fusion. In this approach, the quality of the images was increased by gathering source images and using image-enhancing algorithms. Local sharp derivatives were employed to sharpen the images. Finally, modified independent component analysis was employed to merge images. Zhang et al. [20] implemented an algorithm for integrating two medical images. The algorithm involved the process of dividing source images into LF and HF components using n NSST. LF coefficients were merged using a saliency map, while HF coefficients were combined with improved morphology operations. This approach provided better results for CT in terms of quantitative evaluations.

Framelet Wavelet (FT) based method for image fusion was proposed by Kong et al. [21]. The authors applied FT on the source images to generate multiple subbands. Spatial frequency and guided filter random walks were used to combine these subbands. Inverse FT was applied to obtain the fused image. However, the proposed methods generated images with poor contrast. Sangeetha et al. [22] highlighted the role of DL in image fusion. Input images were preprocessed using image processing techniques to eliminate noise. The preprocessed images were fused using deep neural networks.

## PROPOSED MEDICAL IMAGE FUSION METHODOLOGY

Although a lot of MIF techniques have been developed to date, the fused image quality remains substandard. Although deep networks have attained significant progress in IF, their performance is more excellent than other methods. It is not possible to apply deep networks straight to a spatial domain image without significantly losing certain information. In addition, variations in illumination and contrast have an impact on image fusion, producing a low-quality image. The new MIF approach presented in this research overcomes the aforementioned limitations to produce a fused image that retains all of the information without any loss of it. Figure 1 shows a framework of the suggested MIF approach. The recommended fusion approach consists of the following primary procedures:

- Image decomposition.
- Approximation subbands fusion strategy based on local features.
- Detail subband fusion with DCNN.
- Reconstruction of the fused image.

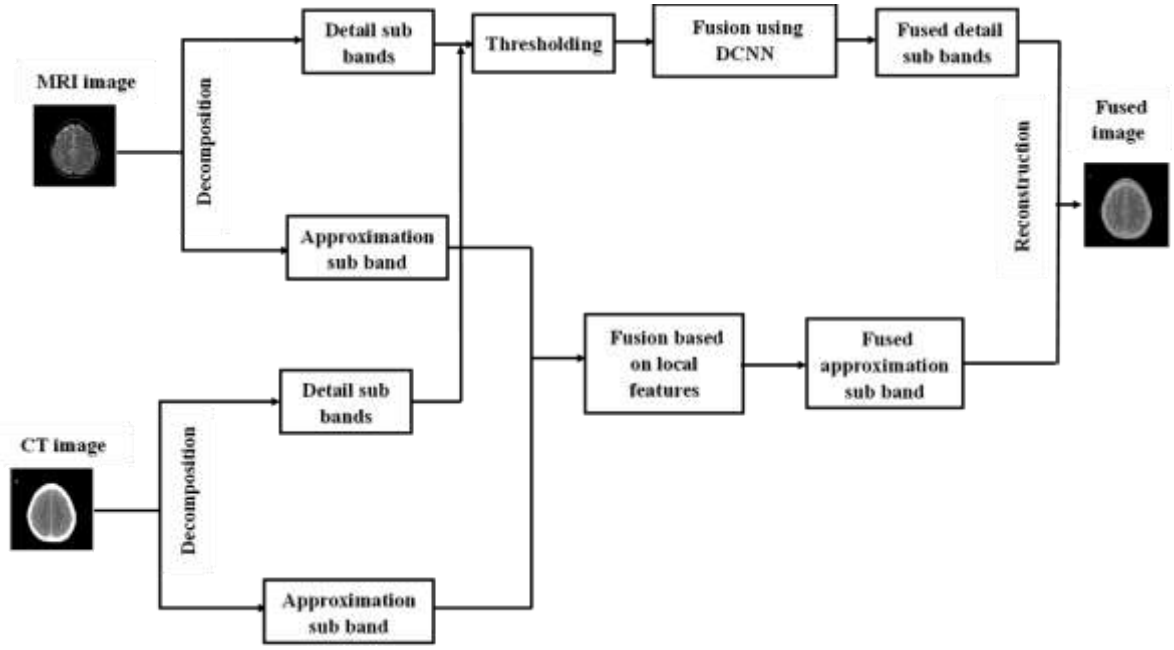


**Figure 1.** The proposed MIF method's framework

## Image decomposition

Wavelet transform is commonly utilized in IF due to its ability to preserve the diagnostic information in both time frequency and divide an image into multiple subbands. WT-based IF methods have been introduced to prevent the limitations of both spatial and frequency domain methods. For each medical image, WT is applied to obtain low-frequency and high-frequency coefficients. Approximation sub-bands are represented by the low-frequency coefficients, while detail sub-bands are shown by high-frequency coefficients. Then, approximation bands of the source image are merged using local features and detail subbands are fused employing the DCNN. The local features fusion aims to improve the visual quality of the fused image and contrast, and the DCNN approach assists in preserving edges, borders, and lines. The whole procedure aims to preserve all feature integrity while transferring information from the source images to the fused image.

After decomposition, noise is found in the detail subbands. This noise can negatively impact the fusion process. So, the noisy pixels should be removed before the fusion process. In this investigation, improved wavelet thresholding methods have been proposed to remove noise and accurately fuse essential features from MRI and CT detail subbands. The proposed threshold function can be expressed as,

$$\widehat{w}_{i,j} = f(x) = \begin{cases} \left( |w_{i,j}| \left( |w_{i,j}| - \frac{T}{\gamma^{\alpha\left(\sqrt{|w_{i,j}|/T-1}\right)}} \right) \right), & |w_{i,j}| < T \\ 0, & |w_{i,j}| \geq T \end{cases} \quad (1)$$

$$T = \sigma_i \frac{\sqrt{2 log n_i}}{\sqrt{n_i}} \quad (2)$$

$$\sigma_i = \frac{MAD(D_i)}{0.6745} \quad (3)$$

$$\text{Mean Absolute Deviation (MAD)} = \text{median}\left(\left|D_j - \text{median}(D_j)\right|\right) \quad (4)$$

Where, α and γ- controlling parameters, n- subband image size, $\sigma_i$-standard deviation

## Fusion of approximation subbands

Let $AS_j^{CT}(x,y)$ and $AS_j^{MRI}(x,y)$ represent approximation subbands of CT and MRI, respectively. $AS_j^F(x,y)$ denote the fused approximation subbands. In this investigation, approximation subbands are merged based on local Average Deviation (AD). The fusion processes are given in Table 1.

**Table 1.** Approximation of subband fusion using local features

**Input:** $AS_j^{CT}(x,y)$ and $AS_j^{MRI}(x,y)$
**Output:** $AS_j^F(x,y)$

**Step 1:** Divide a subband into M X N (3 x 3) local region
**Step 2:** Compute AD for both $AS_j^{CT}(x,y)$ and $AS_j^{MRI}(x,y)$. The AD of CT image can be computed as,

$$AD_j^{CT} = \frac{1}{M\times N} \times \sum_{p=1}^{M}\sum_{q=1}^{N} \left| AS_j^{CT}\left(x+p-\frac{M+1}{2}, y+q-\frac{N+1}{2}\right) - \overline{AS}_j^{CT}(x,y)\right| \quad (5)$$

The AD of MRI image can be calculated as,

$$AD_j^{MRI} = \frac{1}{M\times N} \times \sum_{p=1}^{M}\sum_{q=1}^{N} \left| AS_j^{MRI}\left(x+p-\frac{M+1}{2}, y+q-\frac{N+1}{2}\right) - \overline{AS}_j^{MRI}(x,y)\right| \quad (6)$$

**Step 3:** Normalize AD. Normalized AD (NAD) of CT can be defined as,

$$NAD_j^{CT}(x,y) = \frac{AD_j^{CT}(x,y)}{AD_j^{CT}(x,y)+AD_j^{MRI}(x,y)} \quad (7)$$

$$NAD_j^{MRI}(x,y) = \frac{AD_j^{MRI}(x,y)}{AD_j^{CT}(x,y)+AD_j^{MRI}(x,y)} \quad (8)$$

**Step 4:** Define a Matching Function (MF)

$$MF_j^{CTMRI}(x,y) = \left|NAD_j^{CT} - NAD_j^{MRI}\right| \quad (9)$$

**Step 5:** Define a threshold function, λ
if $MF_j^{CTMRI}(x,y) \geq \lambda$

$$AS_j^F(x,y) = \begin{cases} AS_j^{CT}(x,y), & AD_j^{CT}(x,y) \geq AD_j^{MRI}(x,y) \\ AS_j^{MRI}, & AD_j^{CT}(x,y) < AD_j^{MRI}(x,y) \end{cases} \quad (10)$$

else

$$AS_j^F(x,y) = NAD_j^{CT}(x,y) \times AS_j^{CT} + NAD_j^{CT}(x,y) \times AS_j^{MRI}(x,y) \quad (11)$$

## Fusion of detail subbands

In recent years, DL models have been successfully applied in many fields including computer vision tasks, image classification, object segmentation, and IF [23]. Figure 2 illustrates the structure of the DCNN utilized for merging details subbands. As shown in Figure 2, the proposed DCNN consists of two branches. The detail subbands from CT and MRI images are fed to two branches of the DCNN. Three convolutional layers and one pooling layer make up each branch.

Each convolutional layer has its filter size and stride set at 3x3 and 1, respectively. The layer known as max-pooling is used. The pooling layer's kernel size and stride are set to 2 by 2 and 2, respectively. There are 256 feature maps produced by each branch. The concatenation of these characteristics is sent into the Fully Connected (FC) layer, which is subsequently input into the Softmax layer to create the likelihood of two classes. The network can handle two source images of any size during the fusion process after transforming two FC layers into convolutional ones to create a score map. The feature properties are represented by each coefficient in the score map. The range of each coefficient weight is 0 to 1. By averaging areas, a feature map is obtained from the score map.

After computing feature map N. binary map, b is obtained using the following equation (12),

$$b(x,y) = \begin{cases} -1, & M(x,y) > T \\ 0, & Otherwise \end{cases} \quad (12)$$

There might be some incorrectly categorized pixels in the binary map whose values vary from nearby pixels. To solve this problem, the n x n (n=8) filter is applied to discard singularity points in the feature map. Additionally, artifacts can be generated during the decision map. Guided filtering is applied to resolve this issue. The resultant fused image for detail subbands can be represented as,

$$DS^F = D(x,y)DS^{CT}(x,y) + (1-D(x,y))DS^{MRI}(x,y) \quad (13)$$

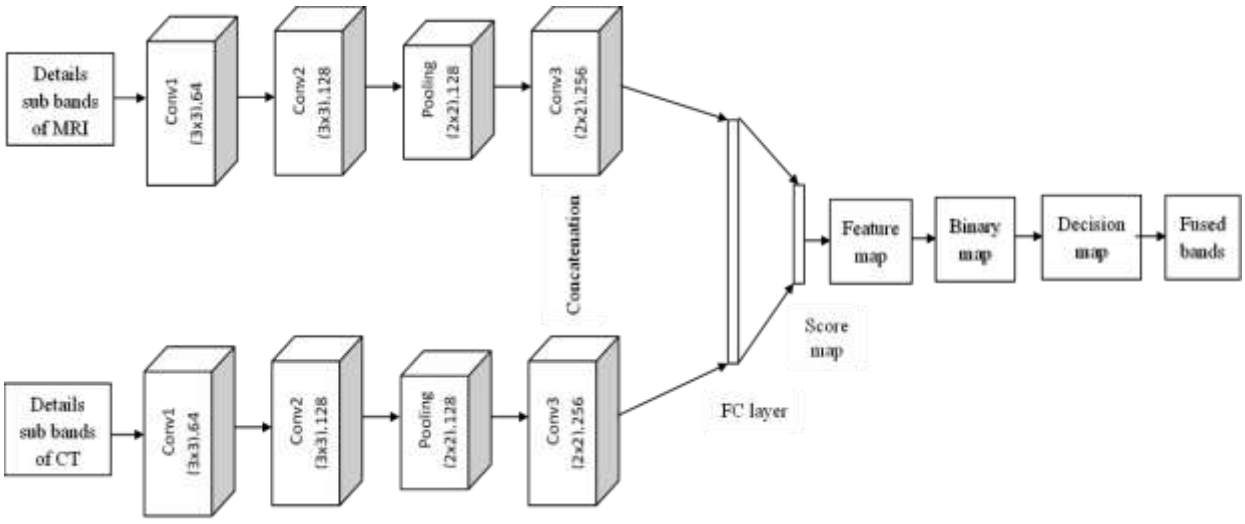


**Figure 2.** Proposed DCNN for detail subband fusion

### 3.4. Image reconstruction

To get the final fused image, the fused detail and approximation subbands are subjected to inverse DWT. The reconstruction process can be expressed as,

$$FF = WT^{-1}(AS^{CT}, DS^{F}) \quad (14)$$

## Experimental results and discussion.experimental setup

In-depth studies using CT and MRI data are carried out to evaluate the effectiveness of the suggested medical image fusion technique. Roughly 190 images are collected from Brain Atlas. The Harvard Medical School built the database [18], which is available to the general public. For experimental purposes, diverse disease images of CT and MRI are taken from the database. Details of medical images used for experimentation are given in Table 2. Notably, all medical images share the same spatial resolution of 512 x 512. Sample images are shown in Figure 3. Experiments are conducted using MATLAB on a laptop equipped with an intel® core i5 processor, CPU at 2.4 GHZ with 12 GB RAM, and Windows 11.

**Table 2.** CT and MRI images used for experimentation

| Dataset | No. of images | Type of source images | Disease |
|---|---|---|---|
| Set 1 | 46 | CT-MRI-T1 | Fatal stroke |
| Set 2 | 52 | CT-MRI-T2 | Meningioma |
| Set 3 | 46 | CT-MRI-T1 | Sarcoma |
| Set 4 | 48 | CT-MRI-T2 | Speech arrest |

| Image type | CT | MRI |
|---|---|---|
| Fatal stroke | 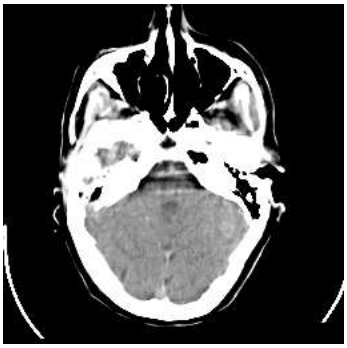 | 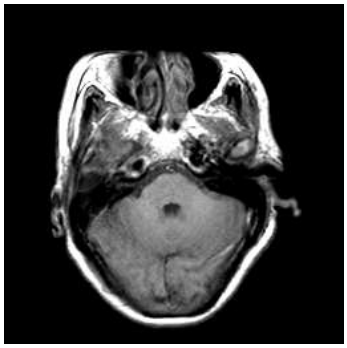 |
| Meningioma | 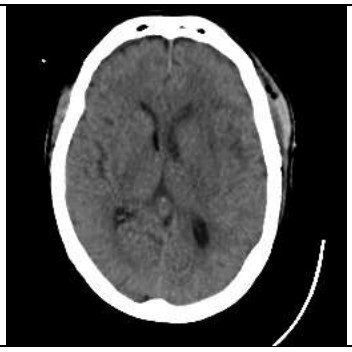 | 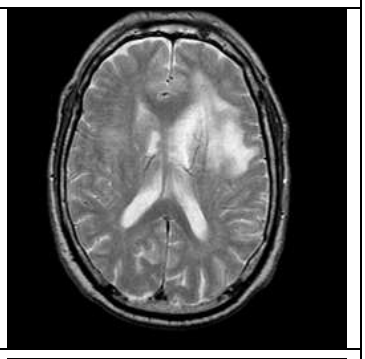 |
| Sarcoma | 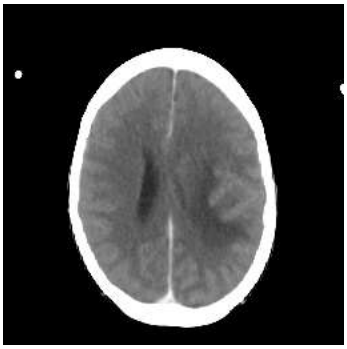 | 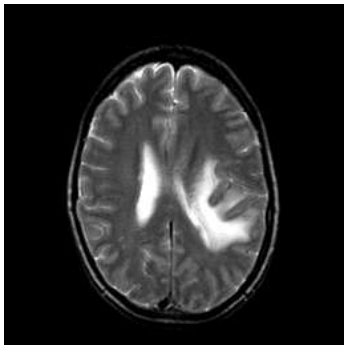 |
| Speech arrest | 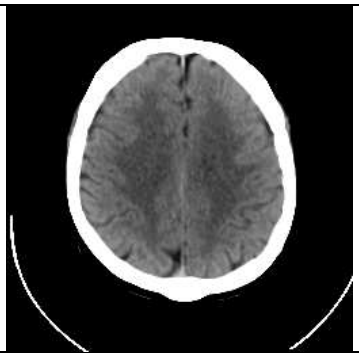 | 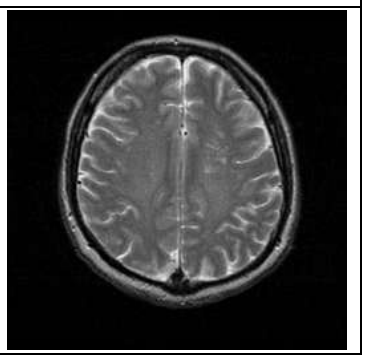 |

**Figure 3.** Example images from the Brain Atlas database

## Metrics

The efficacy of the proposed medical image fusion method is evaluated by computing metrics including Edge Intensity (EI), Normalized Mutual Information (NMI), Standard Deviation (STD), Correlation (C), and Structural Similarity Index Measure (SSIM) [20],[24], [25]. These metrics provide a comprehensive assessment of the developed IF method in light of preserving crucial image features for diagnosis.

## Performance analysis

The proposed IF method has been analyzed in two aspects such as:
(a) Subjective assessment and

(b) Objective assessment

## Subjective assessment

Subjective assessment is the qualitative evaluation of the fused images by human observers. This assessment focuses on the visual quality and diagnostic usefulness of the fused images. The performance of the developed model is assessed and compared with other recent methods reported in the literature including VMD [4], CNN [9], NSST-Xception [11], ResNet [13], and HAM [16]. Information from the initial images should be combined to create a successful fused image. The illustrations of the various IF techniques are shown in Figures 4, 5, 6, and 7. CT and MRI display dense structure and soft tissue information, respectively. The first experiment involves fusing CT images with MRI-TI images of fatal stroke. From Figure 4, it is quite clear that the proposed method demonstrated superior performance by effectively merging information from both CT and MRI images. The other methods like VMD, NSST-Xception, and HAM yielded fused images with poor contrast. Although CNN and Resnet provided better contrast, they failed to preserve edge details.

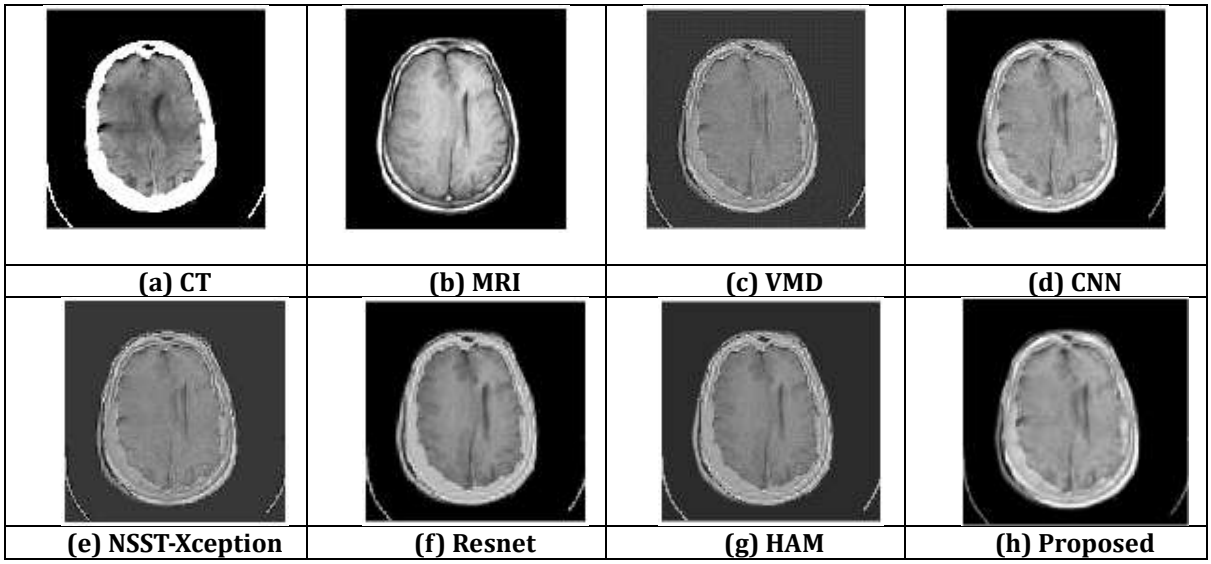


**Figure 4.** Visual analysis of various methods for CT-MRI-T1 (fatal stroke)

In the second experiment, CT and MRI images of meningioma are fused. From Figure 5, it can be noticed that the proposed method successfully transferred information from both the CT and MRI images into fused images with improved contrast and quality. VMD, HAM, and NSST-Xception methods result in fused images with poor contrast. Other methods like CNN and Resnet provided better results. Compared with the approaches mentioned above, the proposed MIF method provided excellent performance with excellent visual quality.

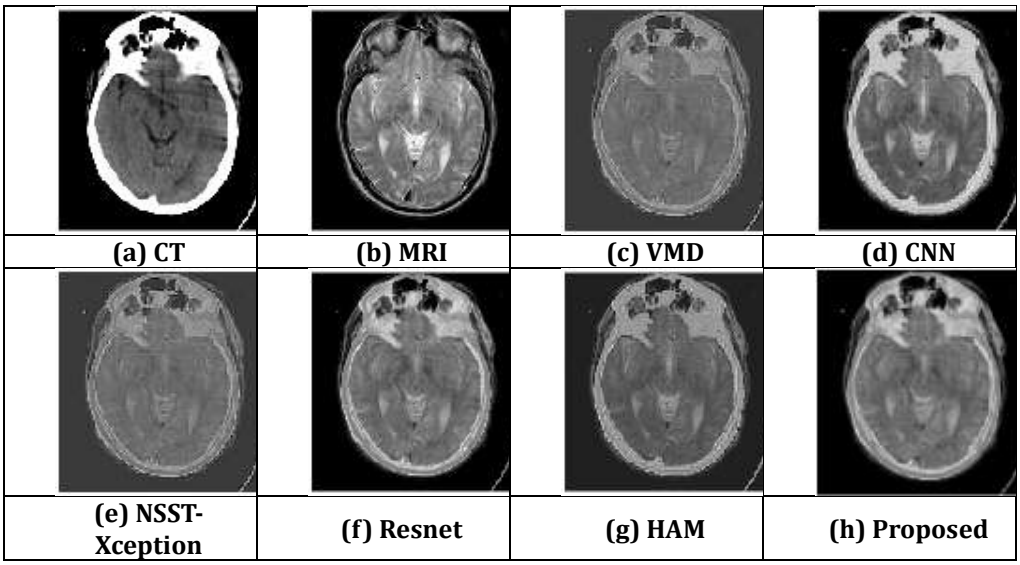

**Figure 5.** Visual analysis of various methods for CT-MRI-T2 (meningioma)

The third scenario evaluates the proposed MIF method's ability to integrate CT and MRI images of sarcoma. Figure 6 illustrates that the proposed method provided better results with good quality and texture information compared to other methods taken for analysis. This effective fusion ensures that no relevant information is lost during the fusion process which allows radiologists to make accurate decisions based on a comprehensive representation of the sarcoma's anatomy.

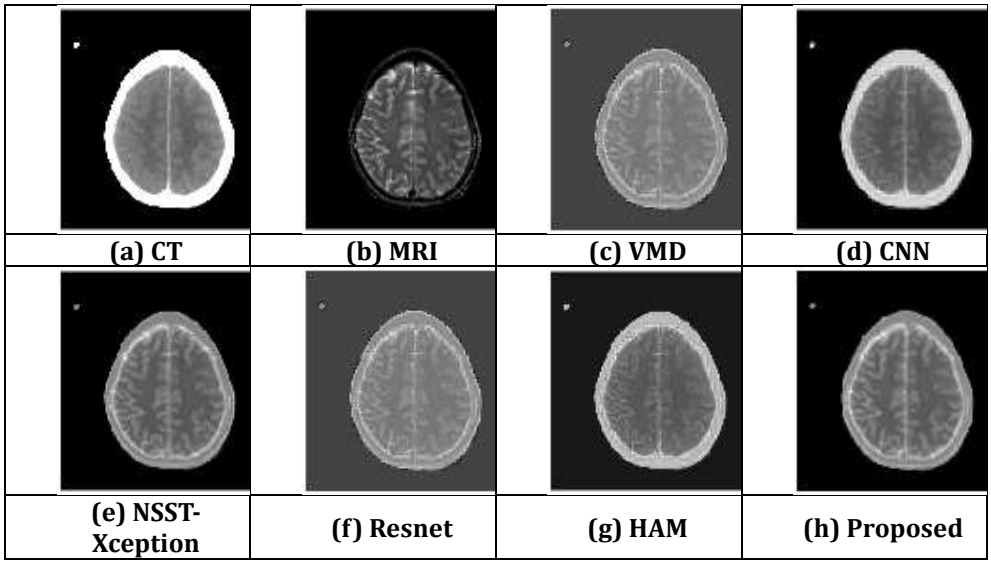


**Figure 6.** Visual analysis of various methods for CT-MRI-T1 (sarcoma)

The fourth experiment used CT and MRI images concerning speech arrest to assess the efficacy of the proposed MIF method. From Figure 7, it is noted that the fusion loss in both VMD and HAM approaches. Similarly, the NSST-Xception method fused MRI and CT images with low contrast. The image with CNN is degraded quality due to fusion loss. Overall, the proposed MIF method retained the necessary information from CT and MRI images for accurate diagnosis.

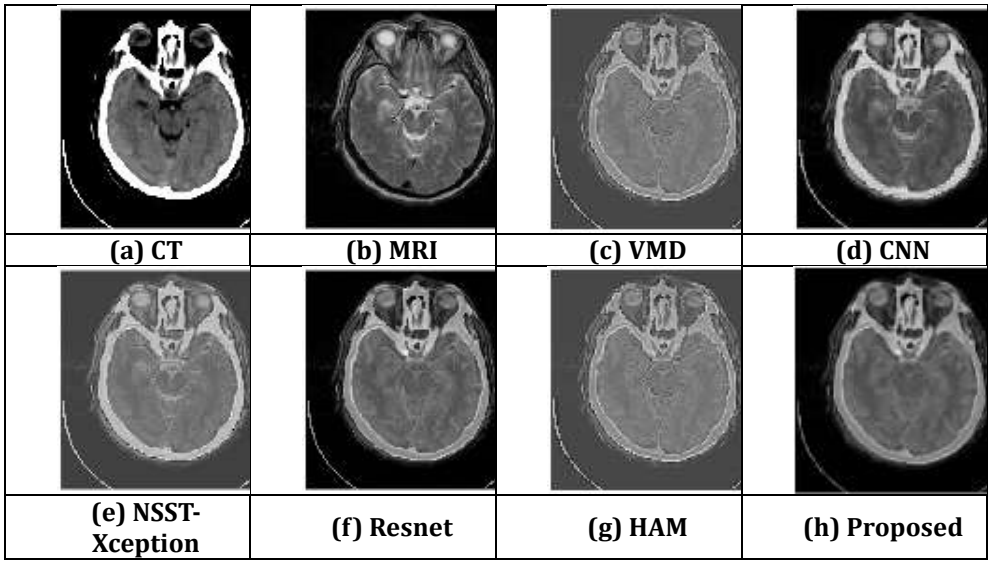


**Figure 7.** Visual analysis of various methods for CT-MRI-T2 (speech arrest)

## Objective assessment

Objective assessment provides quantitative measures of the fused image quality. In this investigation, metrics such as EI, NMI, STD, C, and SSIM are used to objectively analyze the performance of the developed method. The performance of the model is compared with other recent methods reported in the literature including VMD [4], CNN [9], NSST-Xception [ 11], ResNet [13], and HAM [16].

Table 3 compares the performance of the developed method with earlier approaches for CT and MRI image fusion. As depicted in Table 3, the VMD approach gave poor results by achieving lower values for all metrics compared to other methods. The CNN method attained better results with high EI. However, its NMI, STD, C, and SSIM values were lower compared to the developed method. Although HAM methods attained reasonable value for EI, its other metrics are lower, representing the least performance. Resnet demonstrated moderate performance across all metrics with slightly lower compared with the proposed method.

**Table 3.** Comparison of quantitative analysis of various methods for CT-MRI-T1 (fatal stroke)

| Methods | EI | NMI | STD | C | SSIM |
|---|---|---|---|---|---|
| VMD [4] | 70.47 | 0.873 | 65.71 | 0.815 | 0.661 |
| CNN [9] | 94.47 | 0.823 | 64.92 | 0.853 | 0.724 |
| NSST-Xception [11] | 71.77 | 0.844 | 67.23 | 0.837 | 0.722 |
| Resnet [13] | 81.59 | 0.830 | 67.67 | 0.823 | 0.804 |
| HAM [16] | 80.68 | 0.724 | 48.03 | 0.763 | 0.582 |
| Proposed | 95.69 | 0.976 | 73.17 | 0.952 | 0.975 |

Table 4 provides a comparison of different image fusion methods utilized for the fusion of CT and MRI images of meningioma cases. The proposed method showed the highest EI of 93.16 indicating it produces the sharpest edges among all methods. CNN and Resnet performed better results by reporting 86.16 and 84.07, respectively. HAM method had the lowest EI indicating fusion loss. The model attained the highest NMI of 0.970, indicating it has the highest amount of shared information with the source images. HAM method had the lowest STD of 35.01, indicating it generates the least contrast image. The other methods VMD, CNN, NSST-Xception, and Resnet reported STD values of 56.34,58.14,57.55, and 57.42, respectively, suggesting better in contrast. The proposed method posed the highest STD value of 61.83, indicating it gave the fused image with the highest contrast. Similarly, the proposed method demonstrated the highest C of 0.92 and SSIM of 0.985, indicating a high correlation with the source images and preserving the most structural information from the source images. This comparative analysis proved that the developed MIF method not only preserves more information from the source images but also produces images with higher contrast, edges, and better structural similarity.

**Table 4.** Comparison of qualitative results of various methods CT-MRI-T2 (meningioma)

| Methods | EI | NMI | STD | C | SSIM |
|---|---|---|---|---|---|
| VMD [4] | 72.21 | 0.818 | 56.34 | 0.771 | 0.620 |
| CNN [9] | 86.16 | 0.786 | 58.14 | 0.820 | 0.721 |
| NSST-Xception [11] | 73.62 | 0.921 | 57.55 | 0.795 | 0.675 |
| Resnet [13] | 84.07 | 0.848 | 57.42 | 0.784 | 0.710 |
| HAM [16] | 71.17 | 0.758 | 35.01 | 0.720 | 0.642 |
| Proposed | 93.16 | 0.970 | 61.83 | 0.92 | 0.985 |

Comparative analysis of various methods for CT and MRI image fusion is reflected in Table 5. From Table 5, it is noted that the HAM method had the lowest values for EI, NMI, STD, C, and SSIM compared to other methods. VMD and NSST-Xception provided moderate performance in terms of all metrics. Resnet and CNN provided moderate performance by reporting EI values of 89.46 and 95.60, NMI values of 0.866 and 0.931, STD of 59.90

and 58.39, C of 0.896 and 0.921, SSIM of 0.882 and 0.901, respectively. All assessment measures showed that the suggested technique performed better than the other methods, making it an effective technique for CT and MTI image fusion.

**Table 5.** Comparison of qualitative results of various methods for CT-MRI-T1(sarcoma)

| Methods | EI | NMI | STD | C | SSIM |
|---|---|---|---|---|---|
| VMD [4] | 72.51 | 0.828 | 55.29 | 0.783 | 0.598 |
| CNN [9] | 95.60 | 0.931 | 58.39 | 0.921 | 0.901 |
| NSST-Xception [11] | 73.88 | 0.818 | 55.53 | 0.806 | 0.703 |
| Resnet [13] | 89.46 | 0.875 | 59.90 | 0.896 | 0.882 |
| HAM [16] | 70.80 | 0.866 | 38.73 | 0.726 | 0.495 |
| Proposed | 98.02 | 0.984 | 64.60 | 0.977 | 0.985 |

The performance of the new approach for CT and MRI image fusion is compared with earlier methods in Table 6. The new approach seems to perform better than previous methods. This demonstrates how successful the IF-developed strategy is. The proposed method demonstrated the highest values for all metrics, indicating the fused image with high quality, contrast, and structural similarity. CNN and Resnet showed EI of 88.80 and 85.12, respectively. VMD and HAM attained the lowest EI, indicating fewer sharp edges. From the detail analysis, it has been verified that the suggested technique can effectively combine CT and MRI images with good quality, sharp edges, and better structural similarity.

**Table 6.** Comparison of qualitative results of various methods for CT-MRI-T2 (speech arrest)

| Methods | EI | NMI | STD | C | SSIM |
|---|---|---|---|---|---|
| VMD [4] | 66.62 | 0.837 | 60.96 | 0.760 | 0.566 |
| CNN [9] | 88.80 | 0.808 | 49.39 | 0.814 | 0.696 |
| NSST-Xception [11] | 69.61 | 0.950 | 62.47 | 0.785 | 0.689 |
| Resnet [13] | 85.12 | 0.966 | 62.41 | 0.777 | 0.760 |
| HAM [16] | 64.27 | 0.844 | 38.83 | 0.706 | 0.368 |
| Proposed | 94.23 | 0.941 | 67.79 | 0.930 | 0.917 |

## 1. CONCLUSION

This paper has presented a MIF method that combines the merits of each proposed process, including wavelet thresholding, local features fusion, and DCNN to obtain high-quality fuse images for accurate diagnosis. In this approach, wavelet thresholding was used to eliminate noise. A local features-based fusion rule was applied to fuse approximation subbands to improve quality by retaining significant features from the source images. Two branches of DCNN were employed for detail subband fusion. Finally, inverse WT was used to get the fused image. The experimental results revealed that the proposed method gave better visually higher-quality images with better contrast, sharp edges, and structural similarity than other methods of subjective as well as objective assessment. In the future, different imaging modalities will be used to evaluate the effectiveness of the suggested strategy. Other deep learning and hybrid models will be explored to further improve the quality of fused images.

## References

1. B., Y. Xian, D. Zhang, J. Su, X. Hu, & W. Guo. Multisensor image fusion: A survey of the state of the art; Journal of Comput. Communication, 2021, 9, 73-108.
2. Y. Li, J. Zhao, L. Zhihan, & J.Li. Medical image fusion method by deep learning. 2021, 2, 21-29.

3. S. Sandhya, M. S. Kumar, & I. Karthikeyan. A hybrid fusion of multimodal medical images for enhancement of visual quality in medical diagnosis. Proc. of the computer-aided intervention and diagnostic in clinical and medical images, 2019, 61-70.
4. S. Polinati, D. P. Bavirisetti, K. N. Rajesh, & G. R. Naik. The fusion of MRI and CT medical images using variational mode decomposition. Appl. Sci., 2021, 11.
5. Dogra & S. Kumar. Multi-modality medical image fusion based on guided filter and image statistics in multidirectional shearlet transform domain. Journal of Ambient Intelligence. Humaniz. Comput. 2022.
6. N. Tawfik, H. A. Elnemr, M. Fskhr, M. I. Dessouky & F. Samie. Hybrid pixel-feature fusion system for multimodal medical images. Journal Ambient Intelligence Humaniz. 2021.
7. X.Fan, S.Deng, Z.Wu, J.Fan, & C.Zhou. Spatial domain image fusion with particle swarm optimization and lightweight Alexnet for robotic fish sensor fault diagnosis. Biomimetics, 2023, 8(6).
8. K.S. Krishnendu. Multi focus image fusion based on spatial frequency (SF) and consistency verification (CV) in DCT domain. arXiv.2305.11265.
9. J. A. Bhutto, L. Tian, Q. Du, Z. Sun, L. Yu & M. F. Tahir. CT and MRI medical image fusion using noise-removal and contrast enhancement scheme with convolutional neural network. Entropy, 2022, 24.
10. S. Singh, H. Singh, G. Bueno, O. Deniz, S. Singh, H. Mango, P. N. Hrisheekesha & A. Pedraza. A review of image fusion methods, applications and performance metrics. Digital signal processing, 2023, 137.
11. M. Kaur & D.Singh. Multi-modality medical image fusion technique using multi-objective differential evolution based deep neural networks. J Ambient Intell. Human Comput., 12,2021, 2483–2493
12. K. He, D. Zhou, X. Zhang, R. Nie & X. Jin. Multifocus image fusion combining focus region-based level partition and pulse-coupled neural network. Soft. Comput., 2019, 23, 4685-4699.
13. M. Odusami, R. Maskeli unas, R. Damaˇ seviˇ cius, & S, Misra. Explain able deep-learning-based diagnosis of Alzheimer's disease using multimodal input fusion of PET and MRI images. Journal of Medical and Biological Engineering, 2023, 1–12.
14. V.S. Rallabandi & K.Seetharaman. Deep learning-based classification of healthy aging controls, mild cognitive impairment and Alzheimer's disease using fusion of MRI-PET imaging. Biomedical Signal Processing and Control, 80, 2023, 104312.
15. L. Qiu, L. Zhao, R. Hou, W. Zhao, S. Zhang, Z. Lin, H. Teng & J. Zhao. Hierarchical multimodal fusion framework based on noisy label learning and attention mechanism for cancer classification with pathology and genomic features. Computerized Medical Imaging and Graphics, 2023.
16. Y. Wei & L. Ji, Multi-modal bilinear fusion with hybrid attention mechanism for multi-label skin lesion classification. Multimedia Tools and Applications, 2024, 1-27.
17. S. Shilpa, M.R. Rajan, C.S. Asha & L. Shyam, Enhanced JAYA optimization based medical image fusion in adaptive non-subsampled shearlet transform domain. Engg. Sci. Tech. an Int. J., 2022, 35,101245
18. URL: http://www.med.harvard.edu/aanlib/.
19. D. Sale. An enhanced image fusion in the spatial domain based on modified independent component analysis. Multimed Tools Appl., 2022, 81, 44123–44140.
20. Y. Zhang, M. Jin, M., & G. Huang. Medical image fusion based on improved multi-scale morphology gradient-weighted local energy and visual saliency map. Biomed. Signal Process. Control 74, 2022, 103535.
21. W. Kong, Y. Chen. & Y. Lei. Medical image fusion using guided filter random walks and spatial frequency in framelet domain. Sig. Process., 181, 2021.
22. S.B. Sangeetha, S.K. Mathivanan, P.Karthikeya, H.Rajadurai, B.D.Shivahare, S.Malik, & H.Qin. An enhanced multimodal fusion deep learning neural network for lung cancer classification. Systems and Soft Compu., 2024, 6.
23. Y. Li, J. Zhao, L. Zhihan, & Z. Pan. Multimodal medical supervised image fusion method by CNN. Front. Neurosci., 2021, 15.
24. R. Nie, J.Cao, D. Zhou. & W. Qian. Multi-source information exchange encoding with PCNN for medical image fusion, IEEE Trans. Circuits system. Video techno., 31, 2021, 981-1000.
25. A.D. Algarni. Automated medical diagnosis system based on multi-modality image fusion and deep learning, Wire. Pers. Commun., 111, 2020, 1033-1058.